ISSN 1392-2114 ULTRAGARSAS (ULTRASOUND), Vol. 62, No. 2, 2007.

Application of time reversal approach for focusing of Lamb waves

G. Butėnas, R. Kažys

Prof. K. Baršauskas Ultrasound Institute, Kaunas University of Technology
Studentų str. 50, Kaunas, Lithuania, tel. (+370 699 23373)
E-mail: gintas_butenas@yahoo.com

Abstract
In this article an application of ultrasonic time-reversal approach for localization and non-destructive characterization of defects by means of Lamb waves is investigated. The feature of a time-reversed wave field to focus on its source by overcoming dispersion and diffraction effects allows use it for adaptive focusing of Lamb waves. The study of transducers array configuration was performed and showed how it influences wave field focusing patterns in a steel plate.
Keywords: time reversal, Lamb waves, focusing.

Introduction

Application of the ultrasonic time-reversal technique for localization and non-destructive characterization of defects is a powerful tool in modern acoustic. The property of the time-reversed wave field to focus on its source overcoming dispersion and diffraction effects makes it attractive for localization of defects and estimation their geometry in homogeneous or inhomogeneous media with Lamb waves.

The fundamental investigation of the time-reversed wave field focusing was carried out by M. Fink and co-workers [1- 4]. They developed decomposition of the time-reversal operator (DORT) [5] intended for selective focusing and characterization of various scatterers. Comprehensive studies of time-reversal resolution limits were presented in [6]. It is shown in [7] that super-resolution with time-reversal and multiple signal classification (MUSIC) [8] methods can be achieved.

The studies of time-reversed Lamb and other types of guided waves are quite limited, in spite of the fact that non-destructive testing with that type of waves is widespread.

The objective of this investigation was analysis of the time-reversed Lamb wave field focusing in a dispersive range with the purpose to use different Lamb modes in situations where it is not possible to use S_0 mode.

For simulation of the time-reversal process and solution of dynamic equation we are using the commercially available finite element ABAQUS/Explicit software which has a possibility to arrange calculations in a multiprocessing way. In the ABAQUS/Explicit the explicit central difference time integration rule is used to advance the solution. The conditional stability of this approach requires the use of small time increments.

Time-reversal technique

In reference [2] is shown, that propagation of an acoustic pressure field $p(\mathbf{r},t)$ in a lossless medium is described by equation:

$$\vec{\nabla}\cdot\left(\frac{\vec{\nabla}p(\mathbf{r},t)}{\rho(\mathbf{r})}\right)-\frac{1}{\rho(\mathbf{r})c^2(\mathbf{r})}\frac{\partial^2 p(\mathbf{r},t)}{\partial t^2}=0 \qquad (1),$$

where $\rho(\mathbf{r})$ is the density of the medium, $c(\mathbf{r})$ is the speed of sound, $\mathbf{r}$ is the spatial location vector. If the pressure field has a solution $p(\mathbf{r},t)$, then $p(\mathbf{r},-t)$ is also solution invariant to time-reversal. This property is true if the medium has a frequency independent attenuation. If this requirement is not fulfilled, the wave equation will contain odd-order derivatives of t and the invariance to the time-reversal is lost.

Practically, the implementation of the time-reversal idea should is performed in the following way: if the complete three-dimensional sound pressure field from a point like source is recorded with an infinite number of point-like transducers and then time-reversed and re-emitted, the time-reversed pressure field will propagate back to the point source. In practical realization of this approach the re-emitted pressure wave will be $p(\mathbf{r},T-t)$, where T is the duration of the original sound wave.

Time-reversal with linear arrays

The full 3D time reversal cavity described in the previous section is an ideal theoretical construction. In practice, infinite number of receivers has to be replaced by a finite number of transducers which all have a certain, non-zero area. This can be 1D or 2D arrays, either planar or pre-focused. Implementation of 1D linear array, often called a time-reversal mirror (TRM), consists of three steps:

1. Illuminating the target (scattering source) by a plane wave, emitted from one array element.
2. Recording the backscattered sound pressure wave $p(\mathbf{r},t)$ received by all array elements.
3. Re-transmitting the recorded and time reversed wave field $p(\mathbf{r},T-t)$.

Implementation of these three steps in the case of Lamb waves will be presented in the following chapters.

Resolution of time-reversal mirror (TRM)

It is shown in [6] that spatial resolution limits for the homogeneous medium and inhomogeneous medium are different and can be expressed as:

$$g \sim \frac{a}{L\lambda}, \qquad (2)$$

where g is the spatial resolution, a is the aperture length, L is the distance of between the source and the time-reversal mirror, λ is the wavelength (Fig.1). That expression is not exact and is based on roughly approximated parameters. For inhomogeneous media the active aperture is bigger and refers to multiple scattering from different sources:

$$a_e \sim a\sqrt{1+\frac{2\gamma L^3}{a^2}}, \qquad (3)$$

where a_e is the effective aperture length, γ is the inhomogeneous factor. In comparison with traditional techniques, focusing with a time-reversed wave field in inhomogeneous media is more efficient, especially when focusing on objects located further.

That property is useful not only in the case of single layer plates, but also in composite multilayered plates, when it is necessary to detect defects located between different layers.

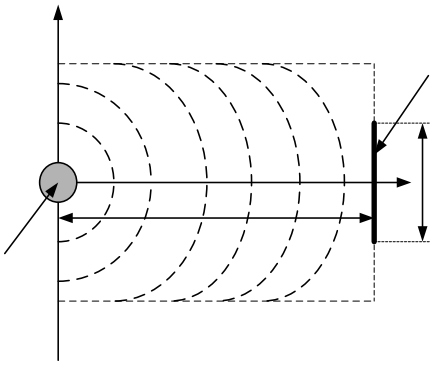

Fig. 1. **TRM source characterization resolution scheme.**

Time-reversal of Lamb waves

Lamb waves are elastic perturbations that can propagate in solid plates with free boundaries. There are two groups of Lamb waves, symmetric and anti-symmetric, that satisfy the wave equation and boundary conditions. Each of the modes can propagate independently of the other modes. The most descriptive way to represent the propagation of a Lamb wave in a particular material is by their dispersion curves, which present the phase and group velocities versus the excitation frequency. The dispersion curves are obtained as the solution of the wave equation. For the symmetric Lamb wave they are described by the equation:

$$\frac{\tan(\sqrt{1-\zeta^2}d)}{\tan(\sqrt{\xi^2-\zeta^2})}+\frac{4\zeta^2\sqrt{1-\zeta^2}\sqrt{\xi^2-\zeta^2}}{(2\zeta^2-1)^2}=0. \qquad (4)$$

For anti-symmetric or transversal motion they are given by:

$$\frac{\tan(\sqrt{1-\zeta^2}d)}{\tan(\sqrt{\xi^2-\zeta^2})}+\frac{(2\zeta^2-1)^2}{4\zeta^2\sqrt{1-\zeta^2}\sqrt{\xi^2-\zeta^2}}=0. \qquad (5)$$

where $\zeta^2=\frac{c_S}{c}$ and $\xi^2=\frac{c_S}{c_p}$ are non-dimensional coefficients; c_p is the phase velocity of Lamb wave, c is the speed of a bulk longitudinal wave, c_s is the speed of a bulk transverse shear wave. Based on Eq.4 and 5 the dispersion curves for 1 mm thickness steel plate were calculated and the results are shown in Fig. 2 and 3. Our attention is directed to A_0 and S_0 modes, which are strongly dispersive in 0-2 MHz range. In that range focusing with traditional techniques is not effective, because the received pulse is distorted by dispersion. Dispersion compensation using the time-reversal method is based on a FILO (first-in, last-out) principle. The wave modes which propagate slowest, after receiving by TRM will be transmitted first, and to the scattering source will come exactly at the same time as the fastest modes.

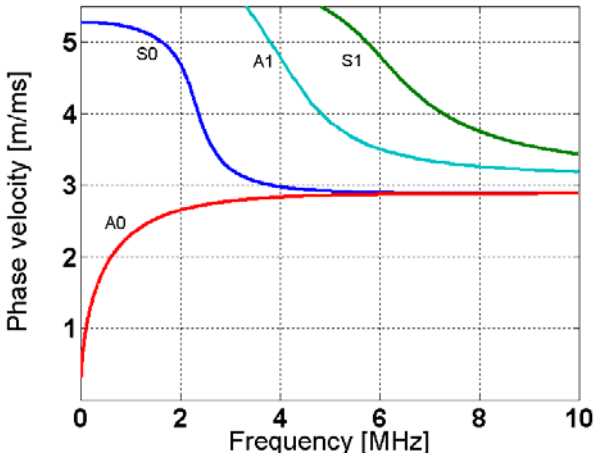

Fig. 2. **Dispersion curves of phase velocities for 1mm thickness steel plate**

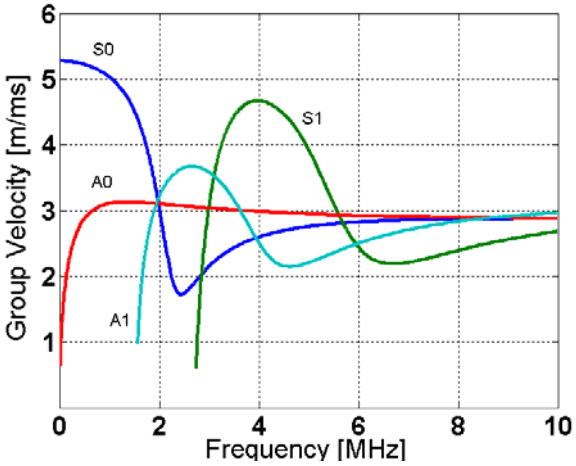

Fig. 3. **Dispersion curves for group velocities 1mm thickness steel plate**

If to assume that the plane of the ultrasonic wave excitation is x_1-x_3, then the displacement field is expressed as:

$$u_i = U_i e^{i\xi(x_1+\alpha x_3-ct)}, \qquad (6)$$

where U_i is the displacement amplitude of corresponding different displacement components, c is the phase velocity, ξ is the wave number along x_1 direction, α is the part of the wave number along x_3 direction.

As it was assumed above, the re-transmitted time reversed wave displacement field is $u(\mathbf{r}, T-t)$ and components for symmetric modes can be expressed as:

$$U(x,z,T-t)=\mathrm{Re}[Ak(\frac{\cosh(qz)}{\sinh(qd)} - \frac{2qs}{k^2+s^2}\frac{\cosh(sz)}{\sinh(sd)})e^{i(kx-\omega(T-t)-\frac{\pi}{2})}] \quad (7)$$

$$W(x,z,T-t)=\mathrm{Re}[-Aq(\frac{\sinh(qz)}{\sinh(qd)} - \frac{2k^2}{k^2+s^2}\frac{\sinh(sz)}{\sinh(sd)})e^{i(kx-\omega(T-t))}]. \quad (8)$$

For anti-symmetric modes:

$$U(x,z,T-t)=\mathrm{Re}[Ak(\frac{\cosh(qz)}{\sinh(qd)} - \frac{2qs}{k^2+s^2}\frac{\sinh(sz)}{\cosh(sd)})e^{i(kx-\omega(T-t)-\frac{\pi}{2})}], \quad (9)$$

$$W(x,z,T-t)=\mathrm{Re}[-Aq(\frac{\cosh(qz)}{\cosh(qd)} - \frac{2k^2}{k^2+s^2}\frac{\cosh(sz)}{\cosh(sd)})e^{i(kx-\omega(T-t))}], \quad (10)$$

where k is the wave number, k_p is the bulk longitudinal wave number, k_s is the bulk transverse shear wave number, ω is the frequency, d is the half-thickness of the plate and $q=\sqrt{k^2-k_p^2}$, $s=\sqrt{k^2-k_s^2}$.

Finite element method modeling setup

The aim of numerical modeling was investigation of the real time-reversal approach implementation problems. Experimental realization of the TRM needs a special equipment for multi-input-output signal processing (receiving, transmitting, reversing in time) and array of ultrasonic transducers. Numerical simulation permits easy change of geometrical configuration of the transducer array and implementation of various signal processing procedures.

The 3D finite element computational model composed of linear elastic elements has been built by using the commercial finite element analysis software Abaqus/Explicit™ (Table 1). In modeling we have used used C3D8R an 8-node plain strain continuum element. Such an element provides a second-order interpolation, with reduced integration and hourglass control (hour-glassing is a numerical phenomenon by which a zero-energy mode propagates through and spoils the solution – see ABAQUS Theory manual [17], Sec. 3.1.1, for more details). Each node has 3-degrees of freedom (plain strain assumption). In mesh control that element is used when average strain is calculated, without second-order accuracy and distortion control. The purpose of the element is to achieve faster computation procedure.

Table 1. **Finite element model data**

Number of nodes	120969
Number of elements	79750
Type of elements:	C3D8R – finite elements with reduced integration CIN3D8 – infinite elements for absorbing boundary
Element linear size	0.5 mm
Element per wavelength	13 elements

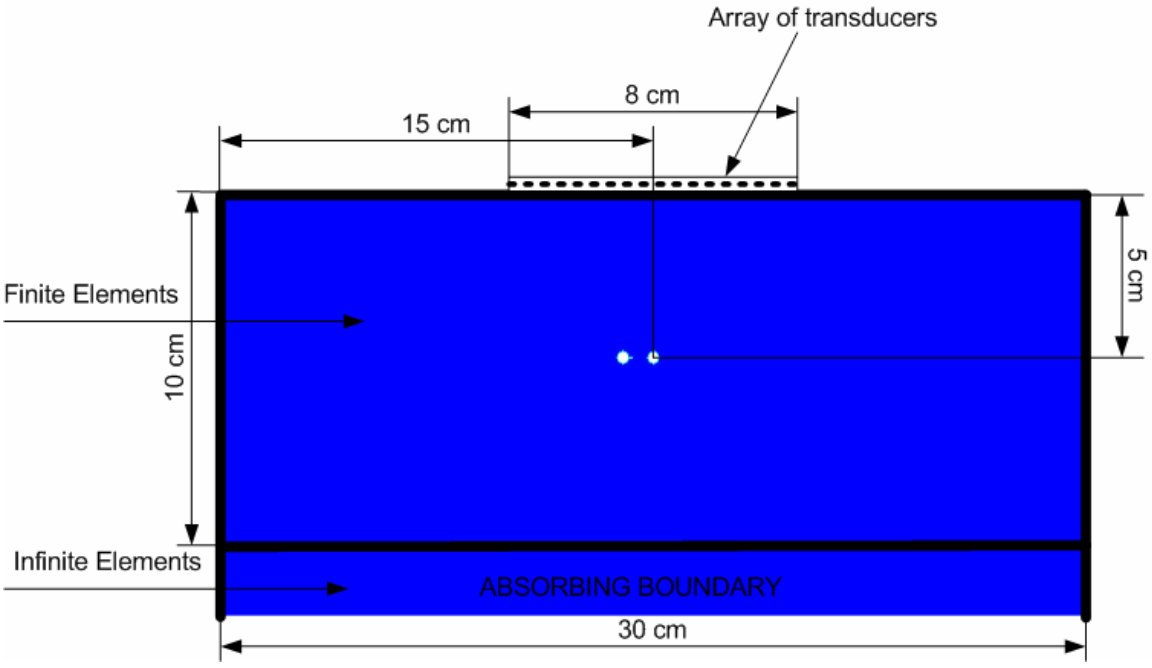

Fig. 4. **Experimental set-up scheme**

The whole assembly is assumed to be a homogeneous elastic steel structure and is modeled using the parameters presented in Table 2.

Table 2. **Material data**

Material	Steel
Density	$\rho = 7800$ kg/m^3
Young modulus	$E = 205.33$ GPa
Poisson's ratio	$P = 0.29$

Table 3. **Transducers array data**

Array length [cm]:	4,8,30
Number of transducers	16,32,64
Transducers spacing	λ/2
Transducer length	λ/3 regular square

The transducers array was assumed a planar 2D array formed by regular square elements.

Excitation parameters

The excitation signal (Gaussian modulated sine burst) is presented in Fig. 5 and is generated in the form of an acoustic pressure at the corresponding node sets. The signal waveform was chosen not accidentally, because this type of signal is widely used in a practice and on the other hand dispersion effects are more noticeable in the case of impulse signals.

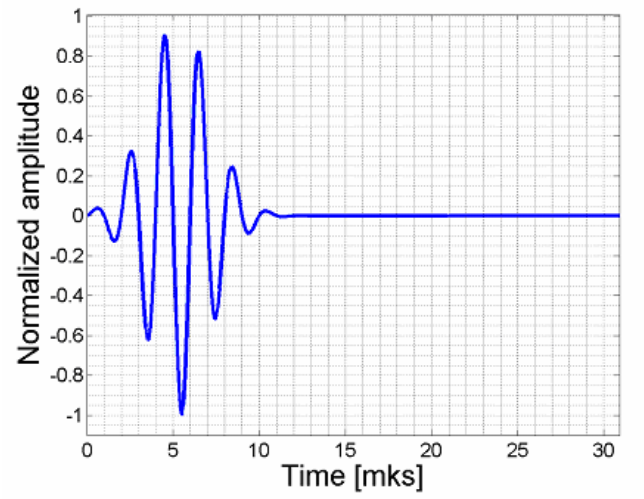

Fig. 5. **The waveform of the excitation signal with the frequency 500kHz used in simulation**

Characterization of a single scatterer using TRM

The first task was investigation of the time reversed Lamb wave focusing in the case of a single scattering source paying the main attention how this focusing depends on the dimensions of the array. The geometry of the simulated structure is shown in Fig. 1. In this case we have not used absorbing boundaries because the TRM should compensate multiple reflections from the edges of the plate. Usually transducers array operates in a pulse-echo mode, but in that case the TRM was realized in a through-transmission mode. It is related, that we exactly know scattering field information and geometrical source configuration. As the scattering source, which imitates a defect, we have chosen a single element located in the middle of the plate edge. The transducers array was placed on the opposite side of the plate. In order to reduce the calculation time we had chosen the same model configuration, but the plate size was reduced to 10x10cm. The signal received at the other end of the plate was time reversed and re-transmitted back. The Fig. 6 demonstrates the directivity pattern of the time-reversed wave field. The directivity depends on the array length and that feature we can exploit for the filtering of different size targets.

If we look to directivity patterns at different distances from the TRM, we can see that wave field refocuses only at exactly defined point (Fig. 7).

This feature can be exploited in the case of multilayered structures, when it is necessary to detect only defects located in a separate layer.

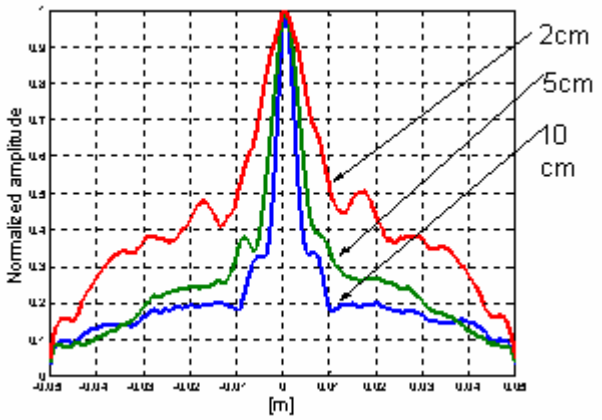

Fig.6. **Directivity pattern for source characterization with different array length**

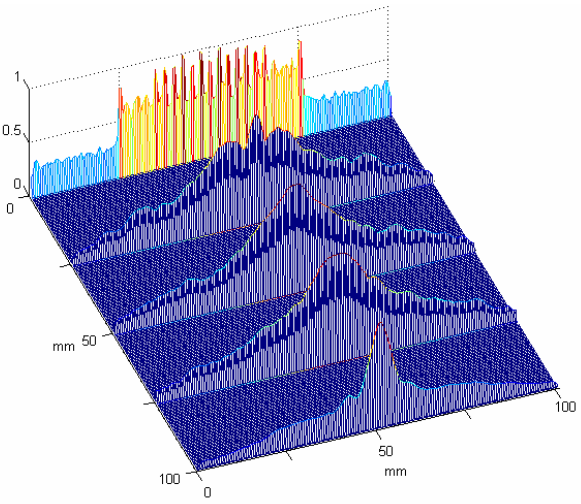

Fig. 7. **Directivity patterns at the distances 2.5, 5, 7.5 and 10 cm from TRM**

Defects characterization using TRM

In the last chapter we have showed that the TRM works properly for a single source characterization in the through-transmission mode. For detection and characterization of two defects we shall use the pulse-echo mode and the model with the geometrical configuration described above. As artificial defects we shall simulate two holes drilled in the middle of a steel plate (Fig. 4 and 8).

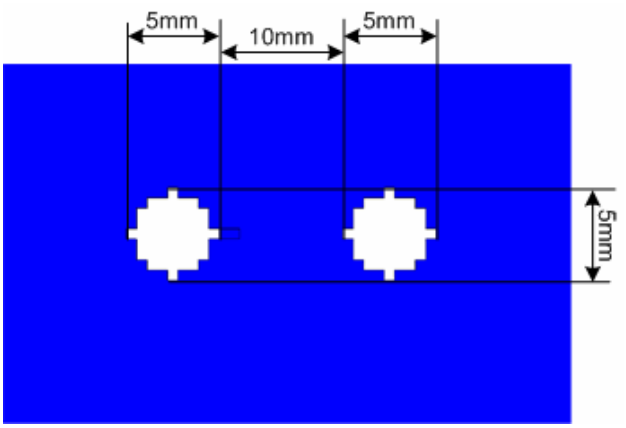

Fig. 8. **Geometrical description of defects**

Refocusing process

The process, which we simulate here, is described in the third chapter. The illuminating pulse is transmitted and reflected by defects. The reflected wave is picked up by the array, reversed in the time domain and re-transmitted back. In the snapshots presented in Fig. 9 we can see the refocusing process in the time domain. The wave field is given as displacement amplitude of the time-reversed Lamb wave. In the last snapshot it is possible to see clearly the location of two defects.

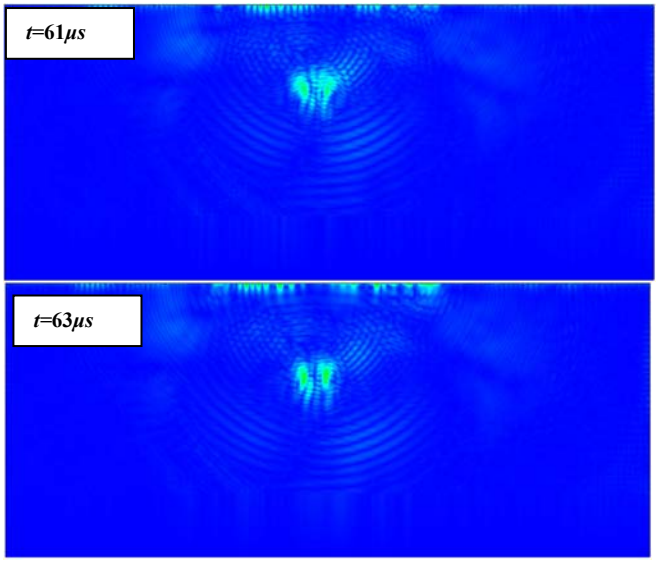

Fig. 9. **Snapshots of the displacement amplitude of the time reversed backward traveling pulse at different time instants**

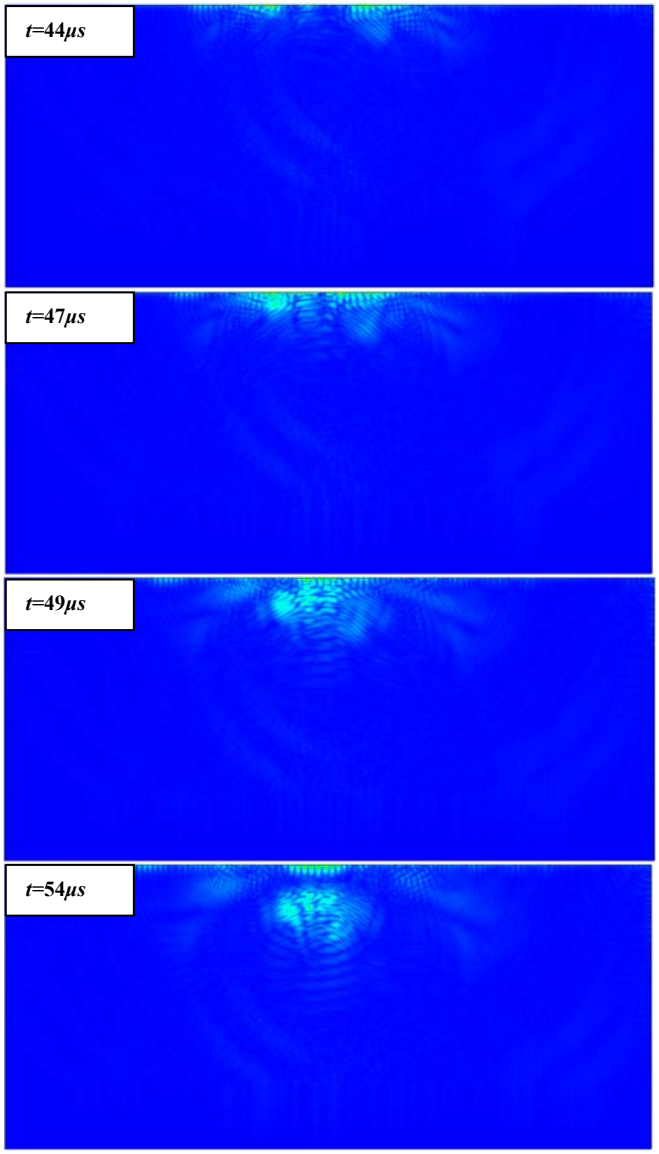

From the wavefield data it is possible to construct the directivity pattern, which is shown in Fig. 10. Here we observe two sharp peaks, whose position and width correspond to positions and dimensions of defects. The exact defect size cannot be extracted directly from that diagram, but the diagram demonstrate the wave field energy distribution, which is caused by defects or scattering sources.

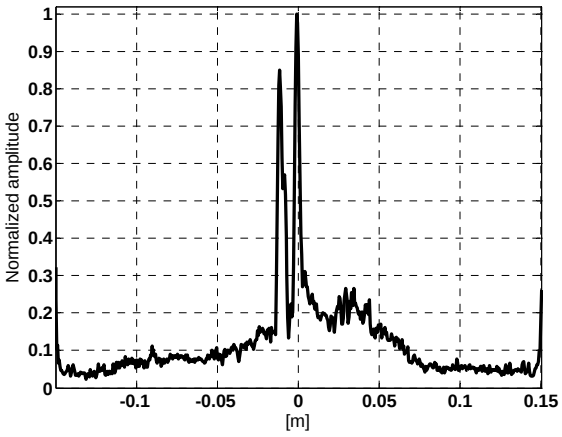

Fig. 10. **Directivity pattern for two defects characterization with TRM**

Conclusions

In this paper application of the ultrasonic time-reversal approach to localization and NDT characterization of defects by means of Lamb waves is investigated. The property of a time-reversed wave field to focus in its source by overcoming dispersion and diffraction effects allows use

this approach efficiently for an adaptive focusing of Lamb waves. The influence of a transducers array configuration on a focusing process was investigated and it was shown how it affects focusing patterns of ultrasonic wave fields.

References

1. **Fink M.** Time reversal of ultrasonic fields – Part I: Basic principles. IEEE Transactions on Ultrasonic, Ferroelectrics and Frequency control. 1992. Vol.39. P. 555-566.
2. **Ing R. K., Fink M.** Time-Reversed Lamb waves. IEEE Transactions on Ultrasonics, Ferroelectrics and Frequency control. 1998. Vol. 45. P. 1032-1043
3. **Fink M.** Time-reversed acoustic. Scientific American. November 1999. Vol. 281. P. 91-97.
4. **Fink M.** Acoustic Time-Reversal Mirrors. Springer-Verlag, Berlin Heidelberg. 2002.
5. **Prada C., Manneville S., Spoliansky D., Fink M.** Decomposition of the time reversal operator: Detection and selective focusing n two scatterers. Journal of Acoustic Society Am. 1996. Vol. 112. P. 411-419.
6. **Borcea L., Papanicolaou G., Tsogka C.** A resolution study for imaging and time reversal in random media. Contemporary Mathematics (2006).
7. **Blomgren P., Papanicolaou G., and Zhao H. Super-resolution in Time-Reversal Acoustic.** J. Acoust. Soc. Am. 2002. Vol. 111. P. 230-248.
8. **Ammari H., Iakovleva E., Lesselier D.** A MUSIC algorithm for location small inclusions buried in a half-space from scattering amplitude at a fixed frequency. Multiscale Modelling Simulation. . 2005. Vol.3P. 597-628.
9. **Delsanto P., Johnson P., Scalerandi M. and TenCate J.** LISA simulations of time-reversed acoustic and elastic wave experiments. Journal of Physics D: Applied Physics. 2002. Vol.35. P.3145-3152.
10. **Wang Ch., Rose J., Chang F. A** Computerized time-reversal method for structural health monitoring. Proceedings of SPIE Conference on Smart Structures and NDE, San Diego, CA, USA. 2003.
11. **Park H., Sohn H., Law K., Farrar Ch.,** Time rReversal active sensing for health monitoring of a composite plate. Journal of Sound and Vibration. 2004.
12. **Prada C., Lartillot N., Fink M.** Selective fFocusing in multiple-targed media: The transfer matrix method. Ultrasonic Symposium.1993. P.1139-1142.
13. **Prada C., Fink M.** Eigenmodes of the time reversal operator: A solution to selective focusing in multiple target media. Wave motion. 1994. P.151-163.
14. **Nunes I., Negreira C.,** Efficiency parameters in time reversal acoustics: Application to dispersive media and multimode wave propagation. Journal of the Acoustical Society of America. 2005. Vol. 117-3. P. 1202-1209.
15. **Barauskas R., Daniulaitis V.** Simulation of ultrasonic pulse propagation in solids. CMM-2003 – Computer methods in mechanics. Gliwice, Poland. 2003.
16. **Predoi M., Sorohan S., Constantin N., Gavan M., Constantinescu D.** Analysis of Lamb wave propagation in steel plate. 22nd Danubia-Adria symposium on experimental methods in solid mechanics. Monticelli Terme/Parma, Italy. 2005.
17. **Abaqus/Explicit™.** v6.3 Theory Manual sec. 3.1.1. 2005.
18. **Wilcox P., Lowe M. and Cawley P.** The effect of dispersion on long-range inspection using ultrasonic guided waves. NDT & E International. 2001. Vol.34. P.1-9.
19. **Wilcox P., Lowe M. and Cawley** P. A Signal Processing Technique to remove the effects of dispersion from guided wave signals. In "Review of progress in QNDE". 2001. Vol. 20. P.555-562.

G. Butėnas, R. Kažys

Laiko apgrąžos metodo taikymas Lembo bangoms fokusuoti

Reziumė

Tiriamas ultragarsinio laiko apgrąžos metodo taikymas defektų vietai ir geometriniams matmenims rasti naudojant Lembo bangas. Tam tinkama laiko apgrąžos metodo savybė kompensuoti dispersiją ir difrakciją. Ištirta ultragarsinių keitiklių gardelės parametrų įtaka Lembo bangų fokusavimui plieno plokštėje.

Pateikta spaudai 2007 06 18

DOI: 10.5755/j01.u.62.2.17025